Modeling of Microwave Heating Systems with Octagonal Tube Cavities: A Comparative Study of Fuzzy-Based and ARX Approaches

Dhidik Prastiyanto[1] , Esa Apriaskar[1]* , Prima Astuti Handayani[2] , Ramadhan Destanto[1], Viyola Lokahita Bilqis[1]

[1] Department of Electrical Engineering, Semarang State University, 50229 Semarang, Indonesia
[2] Department of Chemical Engineering, Semarang State University, 50229 Semarang, Indonesia

* Correspondence: Esa Apriaskar (esa.apriaskar@mail.unnes.ac.id)

Abstract: In the quest to design a robust model for microwave heating systems with symmetrical octagonal tube cavities (MWHSO), a fuzzy-based approach, specifically the Takagi Sugeno Fuzzy Model, was explored to capture the dynamics of the heating process. To achieve this, the mathematical model was adaptively adjusted according to varying input conditions through the utilization of fuzzy logic. Input data were sourced from two magnetrons, with the system outputs derived from measurements acquired from five temperature sensors placed on the heated object. For performance evaluation, the Root Mean Square Error (RMSE) was employed. A comparison was drawn with the autoregressive model with exogenous variable (ARX), a traditional approach wherein the system's mathematical model remains static. Simulation studies were conducted, treating every probe measurement across all dataset validations as distinct cases. It was found that the T-S Fuzzy model surpassed the ARX40 in performance in 33 of the total cases, accounting for 92.49%. The most notable performance of the fuzzy-based approach was observed at a 180-Watt power input, recording an average RMSE of 0.00574 across the five sensors. In contrast, the ARX-based model registered an RMSE of 0.01256. These findings suggest that the fuzzy-based modeling approach presents a compelling alternative for representing the dynamic heating processes within MWHSO.

Keywords: Modeling; Microwave heating; Black-box identification; Model comparison; ARX model; Takagi Sugeno Fuzzy Model

1 Introduction

Microwave heating, due to its capability for volumetric heating, is often perceived as superior to conventional heating methods [1]. Advantages conferred by microwave radiation include reduced energy consumption, selective heating, and improved mechanical properties [2, 3]. These attributes have enticed various industries, such as food, wood, ceramics, and plastics, to adopt microwave heating systems. However, challenges arise from the potential for non-uniform temperature distribution, attributed to the uneven dispersal of microwave power [4]. Such non-uniformities may compromise the internal structure of heated products, thereby diminishing their quality [5, 6]. By employing proficient controllers, the risks associated with heat non-uniformities can be mitigated [1]. It has been suggested that modeling plant dynamics is instrumental in designing controllers that yield satisfactory performance, as it elucidates the temperature profile of the heated product in relation to allocated microwave power, a valuable insight for control design simulations [7, 8].

In the realm of microwave heating dynamics, extensive research has been conducted. Law and Chang [9] embarked on modeling a microwave heating system for oil palm mesocarp with the aim of wastewater reduction. Their three-dimensional model encapsulated the Maxwell Electromagnetic wave equation, water content diffusion equation, and heat conduction equation. Prosuntsov et al. [10] explored both microlevel and macrolevel modeling for polymer composite materials processing via microwaves. Different modeling strategies have been employed by others; Cherbański and Rudniak [11] adopted a differential equations approach, while multiphysical numerical and spectral methods were utilized by Kubo et al. [12] and Navarro and Burgos [13], respectively. These methodologies predominantly hinged on understanding the underlying physics or chemistry characterizing the microwave heating process. Conversely, Yuan et al. [14] championed a departure from this norm by advocating for a black-box

identification system approach, harnessing the ARX method to elucidate the relationship between microwave power and temperatures observed via a probe within the microwave applicator.

Interestingly, despite the proven efficacy of artificial intelligence in various modeling paradigms, its application remains sparing in the context of microwave heating systems. For instance, Saha et al. [15] deployed both AHP and fuzzy logic for soil erosion susceptibility mapping, recording model accuracies of 91.4% and 89.7% respectively. Similarly, Liu et al. [16] utilized fuzzy logic for wind power and wind speed forecasting, leveraging the Takagi-Sugeno Fuzzy Model. This method demonstrated superior performance over other techniques like Support Vector Machine (SVM) and Back Propagation Neural Network (BPNN), underscoring the potential of fuzzy logic in system dynamics modeling.

In light of the aforementioned developments, this investigation delves into modeling a microwave heating system with symmetrical octagonal tube cavity (MWHSO) employing the Takagi-Sugeno Fuzzy logic. This endeavor juxtaposes it against the ARX method, emblematic of prior work concerning black-box identification approaches for microwave heating system modeling. The MWHSO in focus boasts a configuration of two magnetron-driven microwave power generators and five temperature sensors.

The ensuing sections delineate the study's structure. Section 2 elucidates the physical architecture of the MWHSO and the genesis of the models, encompassing both the ARX structure and the proposed fuzzy logic approach. Subsequent section foregrounds the performance results of the proposed model, particularly in juxtaposition with the ARX-derived model, culminating in conclusions and prospects for future investigations on MWHSO system modeling in Section 4.

2 Methodology

2.1 MWHSO System and Design

Typically, a microwave heating system comprises a cavity, a waveguide, and a microwave generator. Within such systems, the microwave cavity serves as the locale for material heating, driven by dipole polarization and ionic conduction resulting from microwave interactions. Concurrently, the waveguide functions as a conduit for electromagnetic waves, guiding them from the microwave generator to the cavity. Essential to the system's function, the microwave generator acts as the power source. For this study, a magnetron, recognized as a prevalent microwave source, was employed.

The chosen cavity design for this investigation was a symmetrical octagonal tube, constructed from materials exhibiting high conductivity, such as aluminum or iron. It has been demonstrated that materials with optimal conductivity enhance the reflection of electromagnetic waves from the magnetron within the microwave cavity, thus ensuring a more efficient heating process. A schematic of the microwave heating system can be referenced in Figure 1.
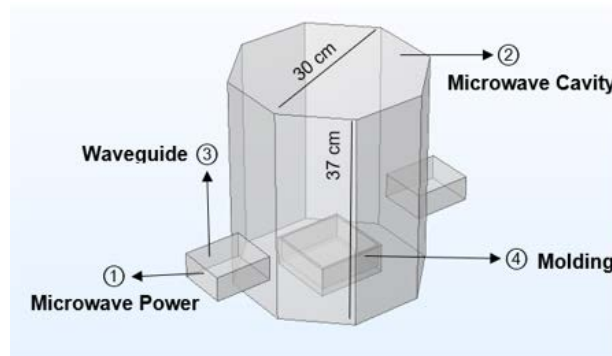

Figure 1. MWHSO design

(1) Microwave power source.

(2) The employed cavity, characterized by a diameter of 30 cm and a height of 37 cm, has previously been evaluated for power efficiency [17].

(3) A WR340 type waveguide, with dimensions of 8.631 cm in width, 4.318 cm in height, and 10 cm in length, was incorporated.

(4) Within the cavity, a container constructed from microwave-transparent material, notably Teflon, measures 12 cm in length, 5 cm in height, and 12 cm in width. This container facilitates the placement of the subject material meant for heating. For real-time monitoring, four sensors are strategically positioned on its sides, with an additional one at its center, enabling temperature assessments of the processed polymer material.

2.2 ARX Model Structure and Design

Among various black-box system structures, the ARX model structure is often regarded as the most straightforward [18]. This structure is delineated by an AR component (Autoregressive) coupled with an additional X component (exogenous input). The AR component elucidates the influence of prior output values on the current output, whereas the X segment emphasizes its dependence on both current and historical input. An equation encapsulating this input-output relationship is depicted in Eq. (1):

$$y(t) + a_{n_a} y(t - n_a) = b_{n_b} u(t - n_b) + \mathrm{e}(t) \tag{1}$$

In this equation, $a_1, a_2, \ldots \in \mathbb{R}^{n_y \times n_y}$, $b_1, b_2, \ldots \in \mathbb{R}^{n_y \times n_u}$ are the coefficient matrices. Parameters n_a, $n_b = \{1, 2, 3, \ldots n, \ldots \in \mathbb{R}\}$, $u(t) \in \mathbb{R}^{n_u}$ and $\boldsymbol{y(t)} \in \mathbb{R}^{n_y}$ represent measured input and output, respectively. The term $e(t)$ signifies the direct error in the difference equation.

Input-output data for the MWHSO were derived from simulations executed on the COMSOL Multiphysics 5.6 software platform. These simulations generated two input values (corresponding to the number of magnetrons) and five output readings from temperature sensors, as depicted in Figure 2. Utilizing a 2.45 GHz frequency, DGEBA (Diglycidyl Ether of Bisphenol A)—possessing a dielectric constant of 3.73 and a dielectric loss factor of 0.68—was subjected to MWHSO-induced heating.
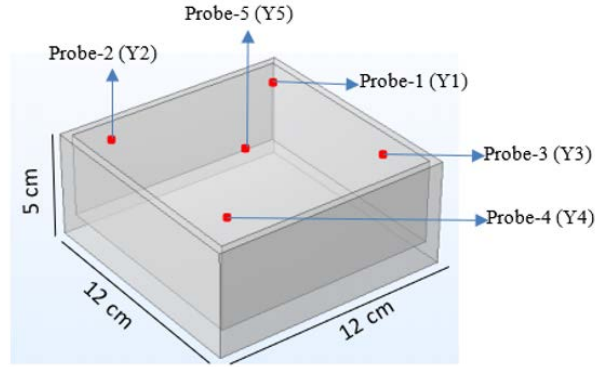

Figure 2. Positioning of temperature sensor probes within the mold

Table 1. Classification of input values for dataset generation

Dataset	Magnetron Power-1 (W)	Magnetron Power-2 (W)	Model Name
IO-20	180	180	ARX20
IO-40	360	360	ARX40
IO-60	540	540	ARX60
IO-80	720	720	ARX80

To assemble the requisite input-output data pairs instrumental for ARX model generation, input signals were modified across four distinct magnitudes: 20%, 40%, 60%, and 80% of the 900-Watt microwave peak power, as detailed in Table 1. Uniform values were designated to both magnetrons to ensure consistent influence on electromagnetic wave distribution. Upon examination of the resultant data pairs, four ARX model candidates emerged. Their efficacy was subsequently evaluated in study [19], where ARX40 was identified as the most apt representation of MWHSO dynamics.

2.3 Takagi-Sugeno (T-S) Fuzzy Model

A dynamic model, delineated in the context of the Takagi-Sugeno Fuzzy Model, is characterized by an array of fuzzy rules of the "IF ... THEN ..." format and a linear dynamic system in the time domain. In this investigation, the dynamic system was represented using the ARX model structure, leading to the derivation of the rule presented in Eq. (2).

i^{th} *rule:*

IF $x_1(t)$ is M_{i1} and $\ldots x_n(t)$ is M_{in} THEN

$$y(t) + a_{n_a} y(t - n_a) = b_{n_b} u(t - n_b) + e(t) \tag{2}$$

where, $x_1(t), \ldots x_n(t)$ denote the operating condition variables, while $M_{i1}, \ldots M_{in}$ symbolize the microwave power input values defining the operational state of the MWHSO. $A(q)y(t)$ and $B(q)u(t)$ were identified as the AR and X components, respectively. By employing a singleton fuzzifier, max product inference, and center average defuzzifier, an aggregate of fuzzy models was formulated, as described in Eqs. (3) and (4).

$$y = \frac{\sum_{i=1}^{r} \omega_i(u) \left(\frac{B_i(q)u(t)}{A_i(q)} + \frac{e(t)}{A_i(q)} \right)}{\sum_{i=1}^{r} w_i(u)} \tag{3}$$

$$\omega_i(u) = \prod_{j=1}^{n} \mu_{ij}(u_j) \tag{4}$$

where, μ_{ij} is recognized as the membership degree from the jth fuzzy set of the ith rule. Given that the coefficient a_i is articulated as in Eq. (5), Eq. (3) transitions to Eq. (6).

$$a_i = \frac{\omega_i}{\sum_{i=1}^{r} w_i} \tag{5}$$

$$y = \sum_{i=1}^{r} a_i(u) \left(\frac{Bi(q)u(t)}{Ai(q)} + \frac{e(t)}{Ai(q)} \right), i = 1, 2, 3, \ldots, r \tag{6}$$

where, the condition $a_i > 0 \in \mathbb{R}$ and $\sum_{i=1}^{r} a_i = 1$ hold true.

In the design of the Takagi-Sugeno Fuzzy model, the MATLAB Fuzzy toolbox function was employed. This model inherently determines the optimal equation from the pre-established ARX models for each distinct operational point. Several input variables were integrated into the fuzzy logic, including the operational condition (OP_COND), alongside variables such as y1(t-1), y1(t-2), y2(t-1), and so forth, up to y5(t-2). Additionally, error models ranging from error1 to error5 were incorporated. Outputs were derived from five sensors, namely temperature 1 (Temp_1) through temperature 5 (Temp_5).

The input variable, OP_COND, indicative of magnetron power, was characterized by four trapezoidal membership functions, as illustrated in Figure 3. Each membership function for OP_COND spanned specific value ranges: 0-270, 270-450, 450-630, and 630-900. The input variables y1(t-1), y1(t-2), y2(t-1), and so forth, up to y5(t-2), each encompassed a singular trapezoidal membership function with a value boundary set between 0 to 250. Conversely, error models from error1 to error5 each had a membership function, trapezoidal in shape, with values ranging from -40 to 40. These selected value parameters were meticulously chosen, considering the intrinsic requirements of each variable. It was observed that deviations to extremely high or low values in these ranges adversely impacted the performance in RMSE metrics. Figure 4 provides an illustrative representation of these membership functions.
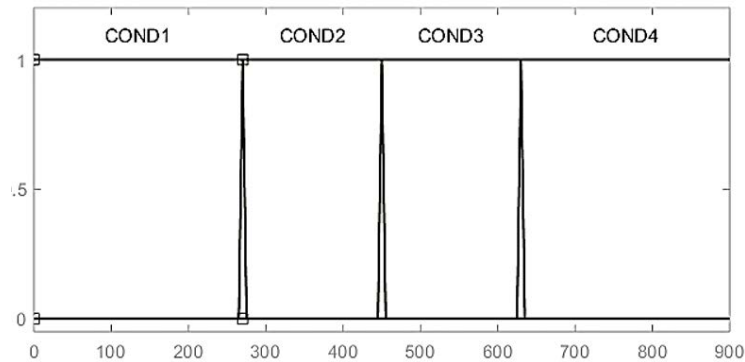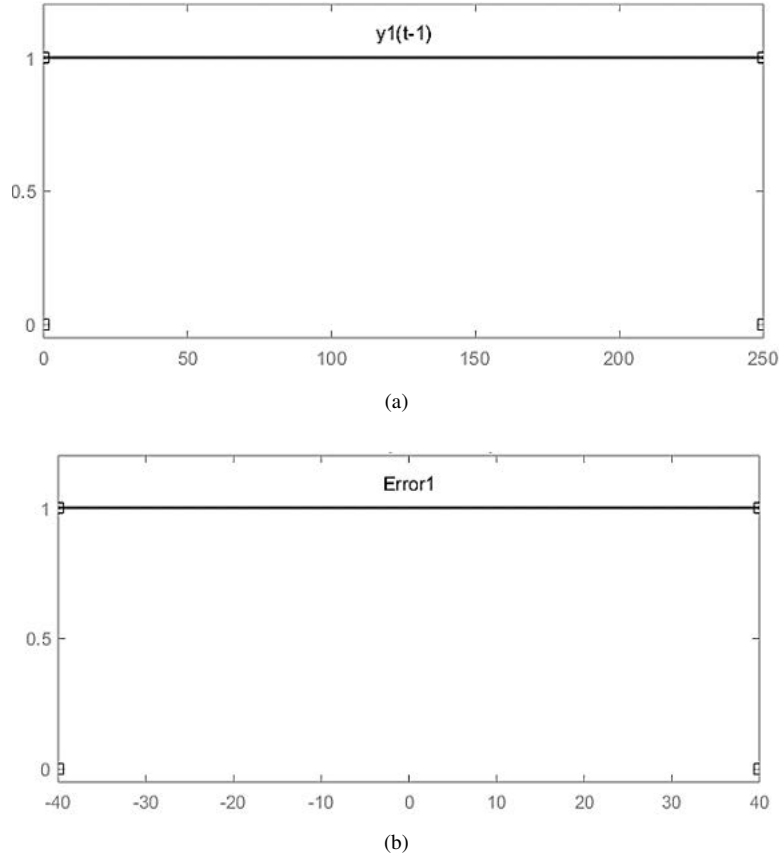

Figure 3. Membership function depiction for OP_COND

(a)

(b)

Figure 4. Membership function illustrations for (a) y1(t-1), and (b) error1

Table 2. Rules formulated for the T-S fuzzy model

Input Variables	Output Variables				
OP COND	Temp 1	Temp 2	Temp 3	Temp 4	Temp 5
COND1	ARX40	ARX20	ARX20	ARX20	ARX20
COND2	ARX80	ARX80	ARX80	ARX80	ARX40
COND3	ARX80	ARX80	ARX80	ARX80	ARX60
COND4	ARX80	ARX80	ARX80	ARX80	ARX60

The fuzzy logic output variables each bore four membership functions aligned with model names outlined in Table 1. Each function assumed a linear form, echoing the ARX Model equation previously utilized in the microwave heating systems' identification. Four distinct rules for this fuzzy model were documented in Table 2.

It was noted that rules predominantly hinged on the OP_COND variable, remaining invariant across all conditions. Subsequent to the crafting of the membership function and pinpointing of the fuzzy rules, the weighted average defuzzification method was applied.

2.4 Model Validation

To assess the efficacy of the devised model, validation was undertaken using the Root Mean Square Error (RMSE) criterion. The methodology to compute the RMSE value is presented in Eq. (7).

$$RMSE = \sqrt{\sum_{i=1}^{n} \frac{(\hat{y}_i - y_i)^2}{n}} \tag{7}$$

where, $\hat{y}_1, \hat{y}_2, \ldots \hat{y}_n$ represent the model outputs, $y_1, y_2, \ldots y_n$ denote the dataset output, and n signifies the dataset size.

The RMSE value was derived through juxtaposing the model equation output with the dataset, which was generated via plant simulations employing the COMSOL Multiphysics 5.6 software. Figure 5 illustrates a block diagram

comparing output values for the calculation of RMSE. Identical perturbation signals, shaped by the microwave power delineated in Table 1, were fed into both the plant and the T-S Fuzzy/ARX models. Subsequently, the resulting model output was compared with the relevant dataset, encompassing all datasets detailed in Table 1.
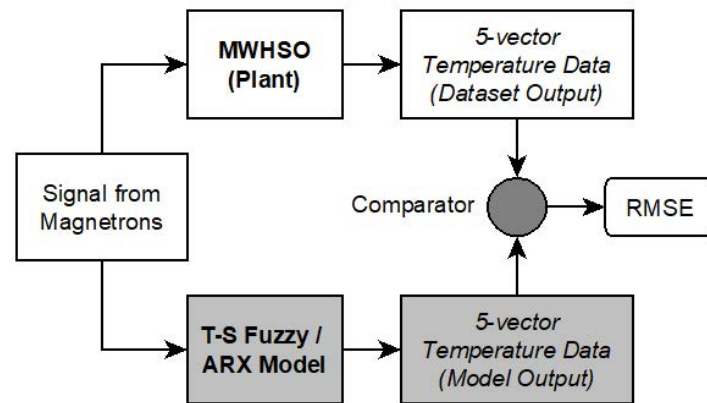

Figure 5. Block diagram illustrating the comparison between the model and the plant

3 Results and Discussion

3.1 Dataset Output Generation

Prior to the modeling of the microwave heating system, simulations were performed to obtain datasets corresponding to specific input-output pairs. As delineated in Table 1, a diverse range of magnetron power levels served as perturbation signals during these simulations. The frequency deployed during these simulations was maintained at 2.45 GHz. Furthermore, the heated material's parameters were characterized by a dielectric constant of 3.73 and a dielectric loss factor of 0.68, epitomizing the attributes of DGEBA. Figure 6 and Figure 7 exemplify dataset outputs derived from perturbation signals of 20% and 80%, respectively.
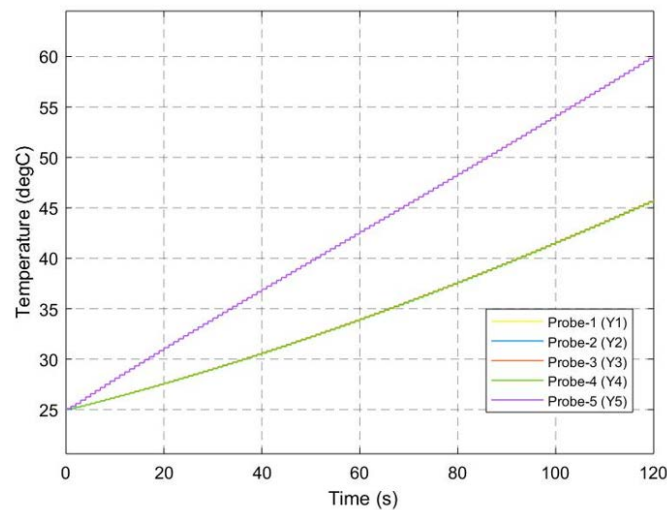

Figure 6. Dataset output IO-20

In Figure 6 and Figure 7, notable temperature variations were observed in Probe-1, Probe-2, Probe-3, and Probe-4, all of which followed a comparable trend. However, Probe-5 displayed a pronounced deviation, attributable to its central placement within the heated object. Microwave heating theory suggests that the initiation of heating transpires from the object's center, radiating outwards [1]. These figures also elucidate the correlation between increased microwave power percentage and an accentuated rate of temperature increase. This is evidenced by the fact that the dataset output IO-80 exceeded $160°C$ after a constant power heating of 120 seconds, whereas the dataset output IO-20 attained a mere $60°C$ over an identical span, commencing from an initial $25°C$.
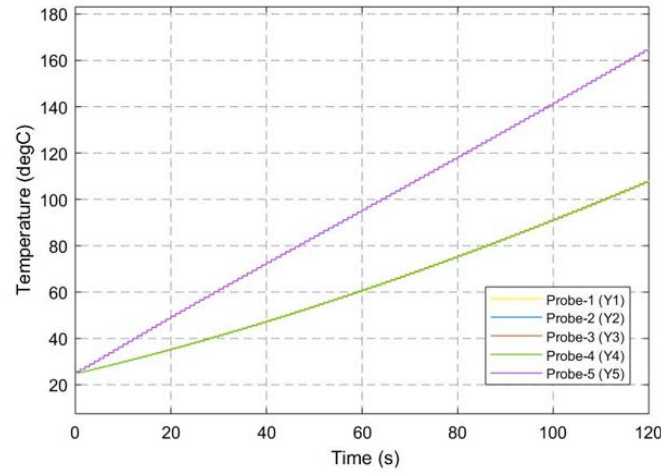
Figure 7. Dataset output IO-80

3.2 Model Validation with Predefined Datasets

Previously, it was noted that the constructed models underwent a comparative analysis with the dataset to assess their capability in mirroring the system's genuine response. The Root Mean Square Error (RMSE) criterion was employed to evaluate the performance of the formulated models for the microwave heating system in alignment with plant dynamics [20]. This criterion effectively gauges the mean disparity between temperatures predicted by the models and the actual values extracted from the datasets. A diminished RMSE value signifies a model's commendable capability to mirror plant characteristics, aligning closely with the dataset.

The comparison presented in Figure 8 illustrates that both the ARX40 and T-S Fuzzy models closely adhere to the IO-60 dataset trend. Although in subgraph (a) of Figure 8 predominantly showcases the response from temperature probe 2, the trend is similarly reflected in other probes, barring probe 5, where a heightened rise is observed, as elucidated in subgraph (b) of Figure 8.

In Figure 9, a more granular distinction between the two models and the foundational dataset is presented. It is evident that the ARX40 model encounters difficulties in mitigating the steady-state error for probe 5. Nonetheless, despite this persistent error in probe 5, the ARX40 model exhibits a marginal advantage over the T-S Fuzzy model, owing to the latter's larger initial error.

Regarding probe 2, an absence of steady-state error was observed in both models. However, the ARX40 model manifested a greater initial error, affirming the relative prowess of the fuzzy model. Insights from Table 3, which catalogs the RMSE data for all probes across predefined datasets, corroborate this. It was discerned that probes 1, 3, and 4 in the IO-60 dataset validation emulate the trajectory of probe 2, with the T-S Fuzzy model consistently outpacing the ARX40.

An intriguing trend evident from Table 3 is the consistent superior mean RMSE values associated with the ARX model across all probes when juxtaposed with the Fuzzy model, even though the disparity between them remains minuscule for a temperature variable, oscillating between 0.002 and 0.013. An exception was observed in the probe 5 of the IO-60 dataset validation, where the RMSE value of the ARX40 was marginally inferior to the Fuzzy model. The widest discrepancy was manifested in the IO-80 dataset validation, which also recorded the highest RMSE values. This insinuates that both models demonstrate compromised efficacy for elevated microwave power input signals. Conversely, with reduced power inputs, both models produced a lower RMSE, with the T-S Fuzzy model's performance in the IO-20 dataset validation being particularly noteworthy, registering an average value of 0.00574.

Table 3. Comparative RMSE metrics for ARX40 and T-S fuzzy model across predefined datasets

Output	IO-20		IO-40		IO-60		IO-80	
	ARX40	Fuzzy	ARX40	Fuzzy	ARX40	Fuzzy	ARX40	Fuzzy
Y1	0.0042	0.0037	0.0083	0.0065	0.0125	0.0077	0.0167	0.0113
Y2	0.0058	0.0038	0.0097	0.0072	0.0152	0.0108	0.0211	0.0144
Y3	0.0116	0.0052	0.0114	0.0099	0.027	0.0106	0.0438	0.0126
Y4	0.0177	0.004	0.0099	0.0075	0.015	0.0118	0.0264	0.0164
Y5	0.0235	0.012	0.0213	0.0178	0.0477	*0.0482*	0.0776	0.0639
Mean	0.01256	0.00574	0.01212	0.00978	0.02348	0.01782	0.03712	0.02372
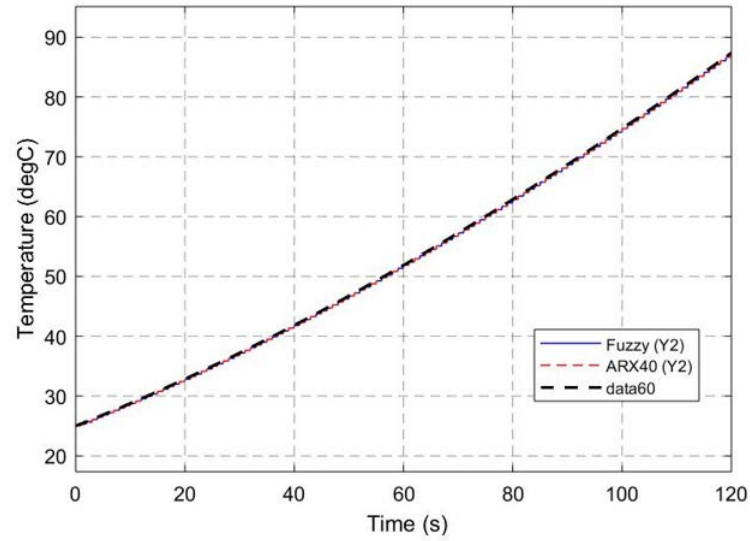
(a)
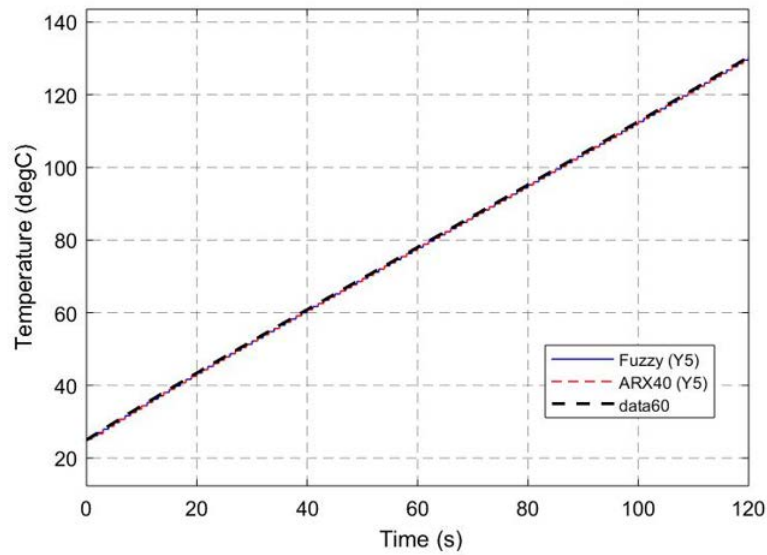
(b)

Figure 8. Comparative visualization of ARX40 and T-S fuzzy model using IO-60 dataset: (a) temperature probe 2 (Y2) and (b) probe 5 (Y5)

3.3 Performance Evaluation Using New Datasets

Subsequent to model validation using predefined datasets, a rigorous assessment was conducted employing alternative datasets. Such datasets were generated using microwave power values not incorporated in Table 1, as delineated in Table 4.

To ensure authenticity, the models were subjected to analogous microwave power input signals as those characterizing the new datasets. Figure 10 represents the response of the models and the system under a 270-Watt microwave power level. Meanwhile, Figure 11 illustrates the disparity in errors between them.

Table 4. Microwave power input values delineating new datasets

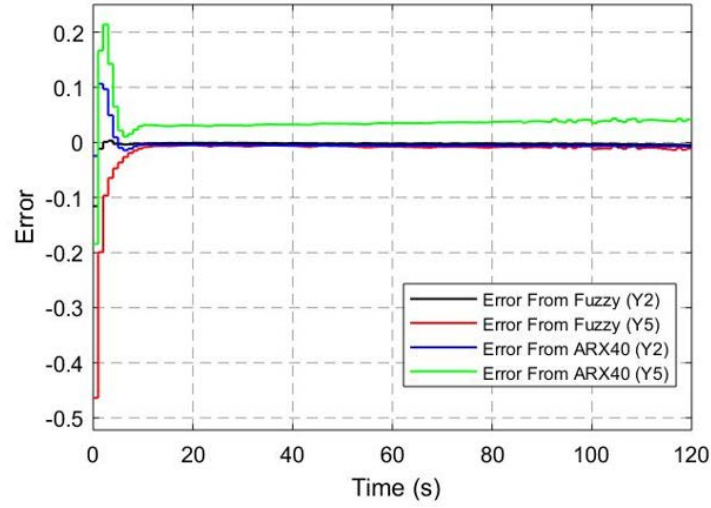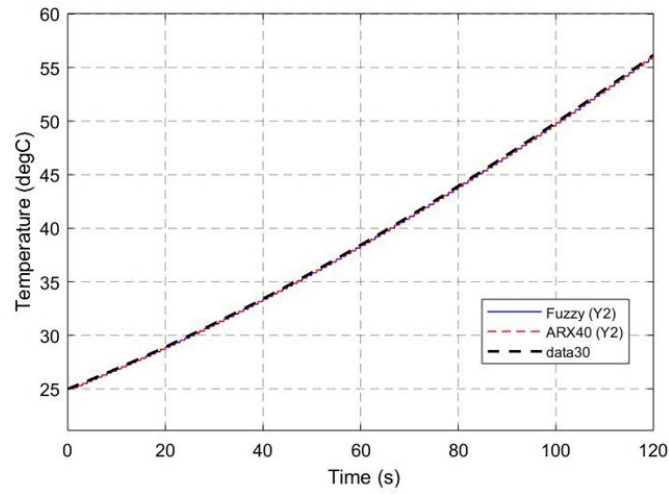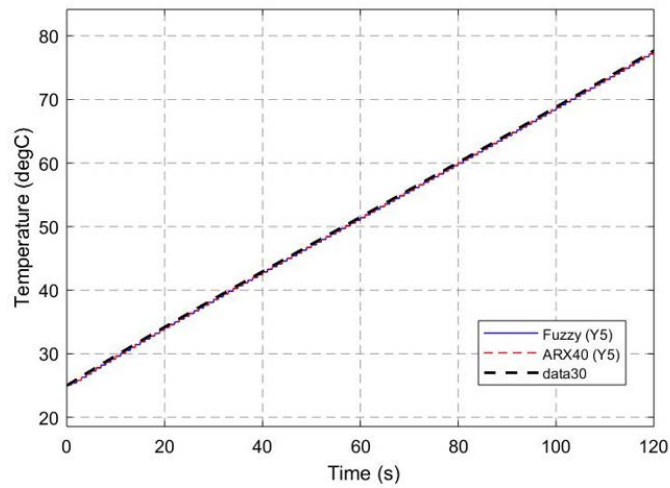| Dataset	Magnetron Power-1 (W)	Magnetron Power-2 (W)	Model Name
IO-30	270	270	ARX30
IO-70	630	630	ARX70
IO-100	900	900	ARX100

Figure 9. Discrepancy assessment between ARX40 and T-S fuzzy model on IO-60 dataset validation

(a)

(b)

Figure 10. Comparative analysis of ARX40 and T-S fuzzy model utilizing IO-30 dataset: (a) temperature probe 2 (Y2) and (b) probe 5 (Y5)
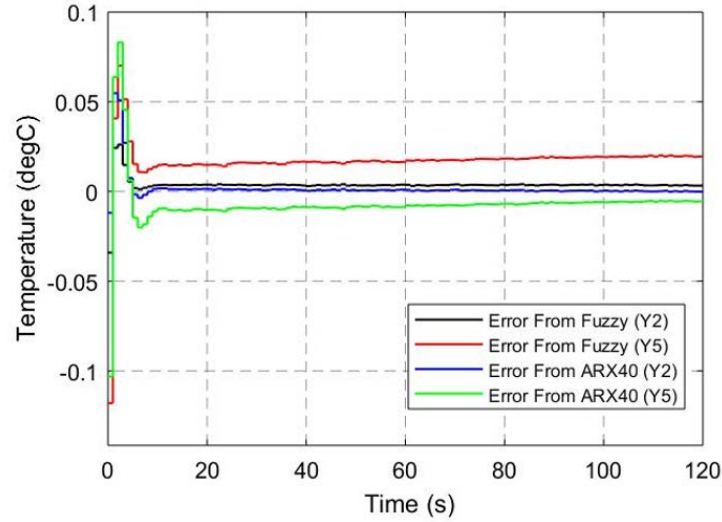
Figure 11. Discrepancy in errors for ARX40 and T-S fuzzy models on IO-30 dataset validation

Table 5. Comparative RMSE metrics for ARX40 and T-S Fuzzy Model across the new datasets

Output	IO-30		IO-70		IO-100	
	ARX40	Fuzzy	ARX40	Fuzzy	ARX40	Fuzzy
Y1	0.0063	0.0061	0.0146	0.0094	0.0209	0.0158
Y2	0.0074	0.0059	0.0181	0.0126	0.0271	0.0180
Y3	0.0075	0.0060	0.0354	0.0115	0.0611	0.0152
Y4	0.0127	0.0059	0.0205	0.0141	0.0391	0.0211
Y5	0.0162	*0.0220*	0.0625	0.0543	0.1080	0.0884
Mean	0.0100	0.0092	0.0302	0.0204	0.0512	0.0317

Upon scrutinizing Figure 10, it was deduced that there was an inconspicuous deviation from the preceding validation phase. Both ARX40 and T-S Fuzzy models adeptly emulated the dataset output for IO-30 dataset validation, with the terminal temperature recorded in probe-5 consistently surpassing other probes. A significant observation from Figure 11 reveals that both models exhibited substantial steady-state errors for probe 5 measurements. Herein, the ARX40 model evidenced a diminished error as compared to the T-S Fuzzy model, suggesting a superior performance by the former. This inference is further fortified by the RMSE values presented in Table 5, wherein the RMSE value associated with probe 5 in the IO-30 dataset, as simulated by ARX40, is marginally reduced in comparison to the Fuzzy model.

Additionally, Figure 11 denotes that the T-S Fuzzy model surpassed the ARX40 in terms of the probe 2 measurements, attributed to a diminished initial RMSE. This observation is congruent with the RMSE values enumerated in Table 5, with corresponding values for ARX40 and T-S Fuzzy standing at 0.0074 and 0.0059, respectively. Analysis of other probes within this dataset, as tabulated in Table 5, reinforced the notion that the T-S Fuzzy model generally maintains a lower RMSE than the ARX40. This suggests that despite the augmented RMSE associated with probe 5, the T-S Fuzzy model, on account of its reduced mean RMSE across all probes, is deemed superior to ARX40.

Consistently, the superior performance of the T-S Fuzzy model over the ARX40, as discerned from prior dataset validations, remains unaltered. The former persists in yielding a reduced mean of RMSE values for all probes compared to the latter. This underscores the efficacy of the T-S Fuzzy model as a more apt representation of the temperature dynamics within the MWHSO system. Further, in the context of probe 5 measurements, the T-S Fuzzy model outperformed the ARX40 in 5 out of the 7 evaluations. Considering each probe measurement across all dataset validations as discrete instances, it can be posited that the T-S Fuzzy model has achieved superiority over the ARX40 in approximately 92.49% of all evaluated cases.

4 Conclusions

In this study, a fuzzy-based model delineating the temperature dynamics of the MWHSO system was meticulously developed. The adoption of the Takagi-Sugeno fuzzy structure was empirically validated to adeptly replicate the datasets. Through rigorous evaluations, it was determined that the T-S Fuzzy model surpasses the ARX-based model,

emblematic of the erstwhile black-box identification paradigm. Out of 35 instances, superiority in performance by the T-S Fuzzy model over the ARX40 model was discerned, as gauged by RMSE values.

From a synthesis of RMSE metrics, a marginal performance discrepancy between the T-S Fuzzy and ARX models was observed. Given this proximate parity in performance, a plausible avenue for future research might encompass a comprehensive assessment of the effectiveness and efficiency of hardware implementations corresponding to both methodologies. Such evaluations hold paramount importance for industrial applications, particularly in the context of the fiscal implications associated with technological deployment.

Moreover, potential expansions in research trajectory could delve into the intricacies of microwave power input modulation. While consistent power levels for both magnetrons were maintained for each operational state in this study, future endeavors might explore the implications of employing divergent power levels. This is particularly pertinent in the domain of selective heating scenarios, underscoring the imperative to facilitate versatile power modulation across the dual microwave generators.

In summation, the findings elucidated herein provide pivotal insights into the temperature dynamics of MWHSO systems, and lay a robust foundation for future investigations geared towards refining and optimizing the existing methodologies.

Data Availability

The data used to support the findings of this study are available from the corresponding author upon request.

Acknowledgements

Conflicts of Interest

The authors declare no conflict of interest.

References

[1] Y. Sun, "Adaptive and intelligent temperature control of microwave heating systems with multiple sources," *Karlsruhe, Germany: KIT Scientific Publishing*, 2016.

[2] I. D. Alonso-Buenaposada, N. Rey-Raap, E. G. Calvo, M. A. Montes-Morán, J. A. Menéndez, and A. Arenillas, "Microwave heating applied to polymer science," in *3rd Global Congress on Microwave Energy Applications*. Cartagena, Spain: Instituto Nacional del Carbon, 2016, pp. 189–191.

[3] T. P. Naik, I. Singh, and A. K. Sharma, "Processing of polymer matrix composites using microwave energy: A review," *Compos. Part A-Appl. S.*, vol. 156, 2022. https://doi.org/10.1016/j.compositesa.2022.106870

[4] J. HouŠová and K. Hoke, "Temperature profiles in microwave heated solid foods of slab geometry: Influence of process parameters," *Czech J. Food Sci.*, vol. 19, no. 3, pp. 111–120, 2013. https://doi.org/10.17221/6586-CJFS

[5] L. Sorrentino, L. Esposito, and C. Bellini, "A new methodology to evaluate the influence of curing overheating on the mechanical properties of thick FRP laminates," *Compos. B Eng.*, vol. 109, pp. 187–196, 2017. https://doi.org/10.1016/j.compositesb.2016.10.064

[6] A. V. Mamontov, V. N. Nefedov, and S. A. Khritkin, "A study of the temperature distribution in a polymer-composite rod when heat-treated with microwave radiation," *Meas. Tech.*, vol. 62, pp. 365–370, 2019. https://doi.org/10.1007/s11018-019-01631-z

[7] A. Triwiyatno, S. Sumardi, and E. Apriaskar, "Robust fuzzy control design using genetic algorithm optimization approach: Case study of spark ignition engine torque control," *Iran. J. Fuzzy Syst.*, vol. 14, no. 3, pp. 1–13, 2017. https://doi.org/10.1088/1755-1315/969/1/012060

[8] E. Apriaskar, D. Prastiyanto, M. A. Malik, A. E. Ramadhan, R. Destanto, H. Abdullah, and M. K. Osman, "Microwave heating control system using genetic algorithm-based pid controller," in *IOP Conference Series: Earth and Environmental Science*. Semarang, Indonesia: IOPScience, 2022.

[9] M. Law and J. Chang, "Modelling microwave heating of an oil palm mesocarp," in *MATEC Web of Conferences*, vol. 240. Cracow, Poland: EDP Sciences, 2018.

[10] P. V. Prosuntsov, S. V. Reznik, K. V. Mikhailovskii, and E. S. Belenkov, "Multiscale modeling of the binder polymer composite materials heating using microwave radiation," in *Journal of Physics: Conference Series*. Suzdal, Russian Federation: Institute of Physics Publishing, 2018. https://doi.org/10.1088/1742-6596/1134/1/012047

[11] R. Cherbański and L. Rudniak, "Modelling of microwave heating of water in a monomode applicator – Influence of operating conditions," *Int. J. Therm. Sci.*, vol. 74, pp. 214–229, 2013. https://doi.org/10.1016/j.ijthermalsci.2013.07.001

[12] M. T. K. Kubo, S. Curet, P. E. D. Augusto, and L. Boillereaux, "Multiphysics modeling of microwave processing for enzyme inactivation in fruit juices," *J. Food Eng.*, vol. 263, pp. 366–379, 2019. https://doi.org/10.1016/j.jfoodeng.2019.07.011

[13] M. C. Navarro and J. Burgos, "A spectral method for numerical modeling of radial microwave heating in cylindrical samples with temperature dependent dielectric properties," *Appl. Math. Model.*, vol. 43, pp. 268–278, 2017. https://doi.org/10.1016/j.apm.2016.10.062

[14] Y. Yuan, S. Liang, J. Zhong, Q. Xiong, and M. Gao, "Black box system identification dedicated to a microwave heating process," in *the 27th Chinese Control and Decision Conference (2015 CCDC)*. Qingdao, China: IEEE, 2015, pp. 4116–4120.

[15] S. Saha, A. Gayen, H. R. Pourghasemi, and J. P. Tiefenbacher, "Identification of soil erosion-susceptible areas using fuzzy logic and analytical hierarchy process modeling in an agricultural watershed of Burdwan district, India," *Environ. Earth Sci.*, vol. 78, pp. 1–18, 2019. https://doi.org/10.1007/s12665-019-8658-5

[16] F. Liu, R. Li, and A. Dreglea, "Wind speed and power ultra short-term robust forecasting based on Takagi–Sugeno fuzzy model," *Energies*, vol. 12, no. 18, 2019. https://doi.org/10.3390/en12183551

[17] D. Prastiyanto, W. Astuti, A. Mahmud, and B. Wijaya, "Design of microwave applicator for processing biomass waste," in *Journal of Physics: Conference Series*. Semarang, Indonesia: IOP Publishing, 2020. https://doi.org/10.1088/1742-6596/1444/1/012016

[18] I. S. Jönsson, "System identification for control of temperature and humidity in buildings," Ph.D. dissertation, Lund University, Sweden, 2015.

[19] D. Prastiyanto, E. Apriaskar, P. A. Handayani, R. Destanto, M. A. Malik, and A. E. Ramadhan, "Identification of microwave heating system with symmetrical octagonal tube cavity using ARX model," in *IOP Conference Series: Earth and Environmental Science*. Semarang, Indonesia: IOP Publishing, 2022. https://doi.org/10.1088/1755-1315/969/1/012025

[20] J. Chen, K. Pitchai, S. Birla, D. Jones, M. Negahban, and J. Subbiah, "Modeling heat and mass transport during microwave heating of frozen food rotating on a turntable," *Food Bioprod. Process.*, vol. 99, pp. 116–127, 2016. https://doi.org/10.1016/j.fbp.2016.04.009